ACCSCIENCE PUBLISHING

Journal of Seismic Exploration

ARTICLE

Thermal damage factors based on thermally induced wave-velocity variation in oil sands

Hui Qi[1], Jing Ba[2]*, Wenhao Xu[2,3], Yuanyuan Huo[1], Jishun Pan[1], Qingchun Jiang[4], and Congsheng Bian[4]

[1]Department of Intelligent Earth Exploration, School of Geosciences and Engineering, North China University of Water Resources and Electric Power, Zhengzhou, Henan, China

[2]School of Earth Sciences and Engineering, Hohai University, Nanjing, Jiangsu, China

[3]BGP INC., China National Petroleum Corporation, Zhuozhou, Hebei, China

[4]Department of Geology, Research Institute of Petroleum Exploration and Development, Beijing, China

Abstract

Oil-sand reservoirs saturated with heavy oil are subject to complex physical and chemical changes under high-temperature conditions. These changes can be quantified using the thermal damage factor, which we evaluated based on Young's modulus and the velocities of P- and S-waves. For the quasi-solid phase of heavy oil-bearing rocks, this method effectively characterizes the degree of rock damage. As temperature increases, heavy oil transitions into a fluid state, reducing rock stiffness. In addition, the thermal expansion of heavy oil weakens the rock matrix and influences the extent of rock damage. We combined an extended Gassmann equation with the Maxwell model for heavy oil to estimate the thermal damage factor. The model was validated using ultrasonic experimental data from rock samples, enabling a quantitative description of the relationship between dry and wet rocks at different temperatures of thermal damage in oil sand. We found that in these rock samples, the temperature-dependent trend of the thermal damage factors can be separated into two stages based on the fluid-viscosity threshold (the liquid point). The porosity of rock samples has no significant influence on this threshold, whereas the viscosities of different fluids affect the threshold value of the thermal damage factor in oil sands. The proposed model provides a theoretical basis for improving the accuracy of reservoir prediction, evaluation, and adjustment, and for optimizing heavy-oil thermal recovery. Furthermore, it offers practical applicability for thermal-recovery monitoring and numerical simulation, enabling more reliable interpretations of temperature-dependent elastic responses.

Keywords: Oil sand; Heavy oil; Temperature; Thermal damage; Gassman equation; Maxwell model

***Corresponding author:**
Jing Ba
(jba@hhu.edu.cn)

Citation: Qi H, Ba J, Xu W, *et al*. Thermal damage factors based on thermally induced wave-velocity variation in oil sands. *J Seismic Explor*. 2026;35(1):33-45. doi: 10.36922/JSE025420092

Received: October 19, 2025

Revised: November 19, 2025

Accepted: November 24, 2025

Published online: December 18, 2025

1. Introduction

With the depletion of conventional reservoirs, unconventional hydrocarbon resources are emerging as the key focus of global petroleum exploration. Heavy oil reservoirs are

a widespread unconventional resource with large potential reserves.[1,2] To enhance the efficiency of exploration and production activities in heavy oil reservoirs, a comprehensive understanding of the basic physical properties of oil sands is required. The exploitation of oil-sand resources usually requires thermal methods, including cyclic steam stimulation, steam flooding, hot water flooding, and steam-assisted gravity drainage (SAGD).[3-6] The core of these methods is to reduce the viscosity of the heavy oil, thus increasing its mobility.[7] However, unconventional hydrocarbon reservoirs are subject to complex physical and chemical changes under high temperatures.[8] These changes can affect the efficiency of oil-sand production as well as the integrity and long-term stability of the reservoirs. This is the primary reason why studying the effects of temperature on the physical properties of heavy oil-bearing rocks is essential.

The effect of high temperature on the mechanical properties of rocks is related to lithology and other physical characteristics.[9-13] Many parameters have been investigated to analyze the influence of temperature on rocks. Dougill *et al.*[14] first proposed the concept of thermal damage. Trippetta *et al.*[15] combined experimental studies and microscopic analyses on saturated carbonate rocks filled with natural hydrocarbons, and found that at low temperatures, the hydrocarbons in the filled rocks were in a solid state. As the temperature increased to 100°C, the solid filler melted, causing the sample's velocity to decrease. The presence of molten hydrocarbons weakened the rock, damaging it and inducing fracturing. At low temperatures, the presence of solid hydrocarbons increased the mechanical properties of hydrocarbon-bearing carbonates. The thermal damage factor (TDF) is used to quantitatively evaluate changes in the mechanical properties of rocks at high temperatures.[16-19] For example, Yang *et al.*[20] conducted experimental studies on thermal damage in limestone. The results indicate that the impact of elevated temperatures on TDF can be directly quantified through the peak compressive strength and the variation rate of the effective solid matrix. As the temperature rises, these properties show a similar exponential trend.

The physical properties and related damage processes of rocks at different scales and depths are not only influenced by rock properties (such as mineral content, porosity, and permeability) but also by temperature, pressure, and pore fillings.[21-23] Heavy oil differs from traditional fluids. It exhibits different properties at different temperatures.[24-25] Butler[26] discussed thermal damage during oil-sand thermal recovery (such as SAGD), especially the dependence of bitumen and mineral properties on high temperature (Gates *et al.*[27]). Similarly, Han[28] studied the thermal damage in oil sands and concluded that heavy oil at high temperature weakens the rock's stiffness. Pang *et al.*[29] pointed out that the pore structure of reservoir rocks changes during steam injection, reducing production. He *et al.*[30] investigated the influence of clay minerals. Despite these studies (see also Yuan *et al.*[31]), there is still limited research on rock damage induced by heavy oil at high temperatures.

In this work, we estimated TDF from ultrasonic data and compared the results with predictions from a viscoelastic Maxwell model combined with an extended Gassmann (EG) equation[32-35] (Carcione's[36] discussion, Section 7.25). Finally, the dependence of thermal damage on temperature and pressure of the oil sands, as well as the thermal damage threshold, was analyzed.

2. Theory

2.1. Thermal damage factor

Zhao *et al.*[37] proposed the definition of TDF for rocks. For rock materials, TDF can be defined using the elastic-strain method, and it is a dimensionless index describing the damage to the microstructure caused by thermal stress and mineral phase changes during thermal recovery.[20,37] In heavy oil sands, heating during thermal recovery alters pore fluids, weakens grain contacts, and may trigger thermally driven microcrack growth. These effects collectively reduce the effective stiffness of the rock skeleton. TDF is therefore important because it provides a quantitative measure of this thermally induced deterioration, enabling the assessment of how temperature-dependent changes in the pore–grain system influence elastic wave velocities and, ultimately, the efficiency and safety of thermal production processes. For an elastic material, the corresponding expression is as follows:

$$\sigma = E_0 \varepsilon_0 \tag{1}$$

where σ, E_0, and ε_0 are the stress, Young's modulus, and strain of the rock in its undamaged state, respectively.

As the rock becomes damaged, we have:

$$\sigma = E_0(1-D)\varepsilon_1 \tag{2}$$

Where $E_T = E_0(1-D)$ is the Young's modulus of the damaged rock, ε_1 is the damaged strain, and D is TDF. Then:

$$D(T) = 1 - \frac{E_T}{E_0} \tag{3}$$

Young's modulus and elastic wave velocity are related as follows:[38]

$$E = \frac{\rho V_P^2 (1+\upsilon)(1-2\upsilon)}{1-\upsilon} \tag{4}$$

Where V_P is the P-wave velocity, υ is the poisson ratio, and ρ is the density.

Combining **Equations 3** and **4**, we obtain the TDF:

$$D(T)=1-\frac{V_{PT}^2\rho_T(1+\upsilon_T)(1-2\upsilon_T)(1-\upsilon_0)}{V_{P0}^2\rho_0(1-\upsilon_T)(1+\upsilon_0)(1-2\upsilon_0)} \tag{5}$$

Where the subscripts T and 0 represent damaged rock at heating temperature and undamaged rock at initial temperature, respectively.

When the temperature varies from room temperature to 160°C, the variations of υ and ρ can be neglected, and TDF can be represented as:[19,20]

$$D_1(T)=1-\frac{V_{PT}^2}{V_{P0}^2} \tag{6}$$

Shear velocity can be defined using a similar approach. Alternatively, in terms of velocities, the Young's modulus can be written as:[38]

$$E=\rho V_S^2\frac{3V_P^2-4V_S^2}{V_P^2-V_S^2} \tag{7}$$

where V_S is the S-wave velocity, and **Equation 5** becomes:

$$D(T)=1-\frac{\rho_T V_{ST}^2(3V_{PT}^2-4V_{ST}^2)(V_{P0}^2-V_{S0}^2)}{\rho_0 V_{S0}^2(V_{PT}^2-V_{ST}^2)(3V_{P0}^2-4V_{S0}^2)} \tag{8}$$

The variation in density with temperature can be neglected, and its influence on stress–strain behavior and TDF estimation is minor. Therefore, density changes do not significantly affect the evaluation of thermal damage trends in heavy oil sands. Hence, we have the TDF simplified to:

$$D_2(T)=1-\frac{V_{ST}^2(3V_{PT}^2-4V_{ST}^2)(V_{P0}^2-V_{S0}^2)}{V_{S0}^2(V_{PT}^2-V_{ST}^2)(3V_{P0}^2-4V_{S0}^2)} \tag{9}$$

2.2. Thermal damage estimation of heavy oil-saturated rocks

Equation 9 indicates that the key parameters affecting the TDF of oil sands are the P- and S-wave velocities. Based on the EG equation,[33,34] we carried out fluid substitution to estimate the TDF of oil sand:

$$\rho_{oi}V_{Poi}^2=K_{oi}+\frac{4}{3}G_{oi} \tag{10}$$

$$\rho_{oi}V_{Soi}^2=G_{oi} \tag{11}$$

Where ρ_{oi} is the density of the oil sand, V_{Poi} and V_{Soi} are the P- and S-wave velocities, respectively, and K_{oi} and G_{oi} denote the bulk and shear moduli, respectively.

Assuming that the porous rock has a uniformly distributed pore structure, we adopt the EG equations here[33-35] (Carcione's[36] discussion, Section 7.25):

$$\frac{1}{K_{oi}}=\frac{1}{K}-\frac{\left(\frac{1}{K}-\frac{1}{K_g}\right)^2}{\phi\left(\frac{1}{K_{if}}-\frac{1}{K_\phi}\right)+\left(\frac{1}{K}-\frac{1}{K_g}\right)} \tag{12}$$

$$\frac{1}{G_{oi}}=\frac{1}{G}-\frac{\left(\frac{1}{G}-\frac{1}{G_g}\right)^2}{\phi\left(\frac{1}{G_{if}}-\frac{1}{G_\phi}\right)+\left(\frac{1}{G}-\frac{1}{G_g}\right)} \tag{13}$$

Where K_g and G_g represent the bulk modulus and shear modulus of the grains, respectively; and K_{if} and G_{if} denote the effective bulk modulus and shear modulus of the pore-filling solid material, respectively; ϕ is the porosity; K and G represent the dry-rock bulk modulus and shear modulus, respectively; and K_ϕ and G_ϕ are dependent on the average deformation of pore volume. When we consider a homogeneous isotropic rock frame, $K_\phi=K_g$ and $G_\phi=G_g$. **Equations 12** and **13** can be expressed as:

$$K_{oi}=K+B \tag{14}$$

$$B=\frac{\left(1-\frac{K}{K_g}\right)^2}{\frac{\phi}{K_{if}}+\frac{1-\phi}{K_g}-\frac{K}{K_g^2}} \tag{15}$$

$$G_{oi}=G+C \tag{16}$$

$$C=\frac{\left(1-\frac{G}{G_g}\right)^2}{\frac{\phi}{G_{if}}+\frac{1-\phi}{G_g}-\frac{G}{G_g^2}} \tag{17}$$

Where the B and C are the pore moduli.

As a viscoelastic medium,[39] heavy oil exhibits three distinct phases depending on temperature: fluid, quasi-solid, and solid. Moreover, heavy oil has liquid and glass points.[40] Due to its high shear viscosity, heavy oil acts as part of the frame (skeleton) when the temperature is below the glass point. At elevated temperatures, however, its viscosity decreases significantly, and it is considered to be a fluid that exerts no influence on the rock frame.[40-42] Given that heavy oil in the solid phase exhibits a finite shear modulus and its viscoelastic properties are frequency-dependent, it

is reasonable to consider them in the frequency domain. Therefore, we adopted the Maxwell model to characterize the temperature- and frequency-dependent complex shear modulus, as it effectively captures the combined elastic and viscous behaviors of heavy oil:[31,33,43]

$$G_{if} = \frac{i\eta\omega}{\frac{i\eta\omega}{G_\infty}+1} \tag{18}$$

$$K_{if} = K_f + \frac{5}{3}G_{if} \tag{19}$$

Where G_∞ denotes the shear modulus of the fluid within the high-frequency range, K_f represents the bulk modulus corresponding to the pore fluid, ω is the angular frequency, i is defined as the imaginary unit, and η represents the viscosity of the fluid that varies with temperature.

For dry rock, its bulk modulus and shear modulus are:

$$K = \rho_{dry}V_{Pdry}^2 - \frac{4}{3}G \tag{20}$$

$$G = \rho_{dry}V_{Sdry}^2 \tag{21}$$

Where ρ_{dry} is density, and V_{Pdry} and V_{Sdry} are the velocities of P- and S-waves in dry rocks, respectively.

Equation 9 was used to obtain the TDFs of the dry rock at varying temperatures, relying on the measured P-wave and S-wave velocities of the dry rock. The damage in dry rock with increasing temperature is primarily caused by differential thermal expansion of mineral grains and microcrack propagation. As temperature rises, mismatched expansion between grains induces stress at grain boundaries, leading to the initiation and growth of microcracks, which progressively degrade the rock's elastic properties.[44] Then, the TDF was estimated using **Equations 9 – 19** as:

$$D_{roi}(T) = 1 - \frac{\rho_{dry}V_{Sdry}^2 + C}{\rho_{dry0}V_{Sdry0}^2 + C_0}FH \tag{22}$$

Where:

$$F = \frac{B - D_{dry}(T)\rho_{dry0}V_{Pdry0}^2 - \frac{1}{3}\rho_{dry0}V_{Pdry0}^2}{B_0 - \frac{1}{3}\rho_{dry0}V_{Pdry0}^2} \tag{23}$$

$$H = \frac{B_0 + \rho_{dry0}V_{Pdry0}^2 + \frac{1}{3}\rho_{dry0}V_{Sdry0}^2 + \frac{5}{3}C_0}{B + \rho_{dry0}V_{Pdry0}^2 - D_{dry}(T)\rho_{dry0}V_{Pdry0}^2 + \frac{1}{3}\rho_{dry}V_{Sdry}^2 + \frac{5}{3}C} \tag{24}$$

And $D_{roi}(T)$ and $D_{DRY}(T)$ are the TDFs of the rock saturated with heavy oil and dry rock at varying temperatures, respectively.

The workflow is presented in Figure 1. The main parameters involved included the measured velocities and density of dry rock, as well as the pore moduli (B and C) of the heavy oil-saturated rock. To calculate these moduli, we initially calculated the bulk modulus of the matrix based on its mineral composition K_g, and then the fluid properties at the corresponding temperature. The porosity ϕ was a known input parameter of oil sands. These parameters were substituted into **Equations 15** and **17** to obtain the

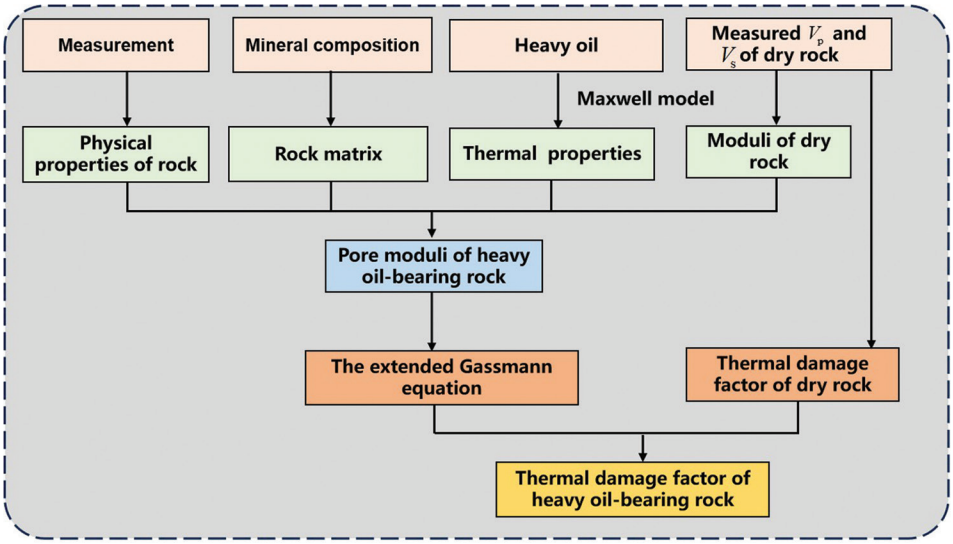

Figure 1. Workflow for estimating the thermal damage factor of oil sands at different temperatures

Table 1. Physical properties of oil sands

Rock type	Density (kg/m³)	Porosity (%)	Grain density (kg/m³)	Mineral bulk modulus (GPa)	Mineral shear modulus (GPa)	Heavy oil (API)	Pore pressure (MPa)	Study
1	1,981	41	2,650	36	44	7.5°	2.3	Yuan *et al.*[31]
2	2,030	38	2,650	36	44	7.5°	2.3	Yuan *et al.*[31]
3	1,890	41	2,490	18	21	6.6°	0	Li *et al.*[41]
4	1,960	36	2,490	18	21	6.6°	0	Li *et al.*[41]
5	1,970	42	2,660	21	24	6.6°	0	Li *et al.*[41]
6	2,045	37	2,650	36	44	9.2°	2.4	Han *et al.*[25]
7	1,980	32	2,431	22	24	6.9°	3.5	Li *et al.*[45]

pore moduli at different temperatures, and then we used **Equations 22-24** to obtain the TDF.

3. Thermal damage factors of oil sands

Here, five oil sand samples (Samples 1, 2, 3, 4, and 5) were selected for analysis. The main mineral components of the samples (Samples 1 and 2) tested by Yuan *et al.*[31] were quartz, and the pore fluid was heavy oil with a 7.5° American Petroleum Institute (API) density and 50°C liquid point. When the temperature rose above the liquid point, the heavy oil behaved as a fluid. The shear modulus of the heavy oil approached zero at approximately 50°C under ultrasonic frequencies, at which point its viscosity was approximately 1,000 cP. During the experimental process, the pore pressure was set to 334 psi. The other samples (Samples 3, 4, and 5) were reported by Li *et al.*[41] The main minerals were quartz and clay. The pore fluid was heavy oil with a 6.6° API density and 48.7°C liquid point. During the test, the pore pressure was zero. Table 1 lists the samples' specific properties.

3.1. Effect of temperature on thermal damage factor

Understanding fluid properties is critical for analyzing the behavior of oil sands. Figure 2 depicts the relationship between the moduli and temperature for heavy oil in all samples and water. As the temperature decreases, the moduli of heavy oil increase. At low temperatures, the finite shear modulus of heavy oil must be taken into account, which makes the properties of oil sands different from those of conventional rocks. At higher temperatures, the shear modulus can be almost neglected and treated similarly to that of water, whereas the bulk modulus decreases with increasing temperature. Because the oil is highly viscous and dense, heavy oil-bearing rocks are more sensitive to temperature changes at low temperatures.[46]

Next, we considered TDF based on **Equation 9**, compared to the results of **Equation 6** (P-waves). Figure 3 shows D_1 and D_2 for the two samples. As can be seen, the values increased with increasing temperature. D_1 was lower

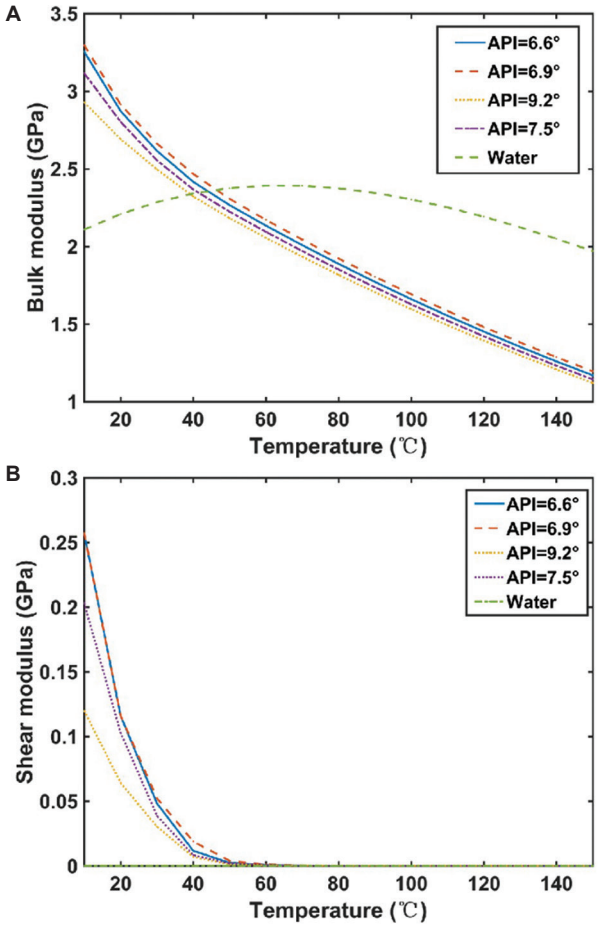

Figure 2. The (A) bulk and (B) shear moduli as a function of temperature for heavy oil and water

than D_2 at low temperature, and the difference decreased with decreasing temperature.

Next, we considered the TDF (D_2) based on **Equation 9**. Figure 4 shows the TDFs for four samples. As can be seen, TDF increased with increasing temperature. In the comparison, at low temperatures, Sample 3 exhibited a higher TDF value compared to Sample 1, indicating that

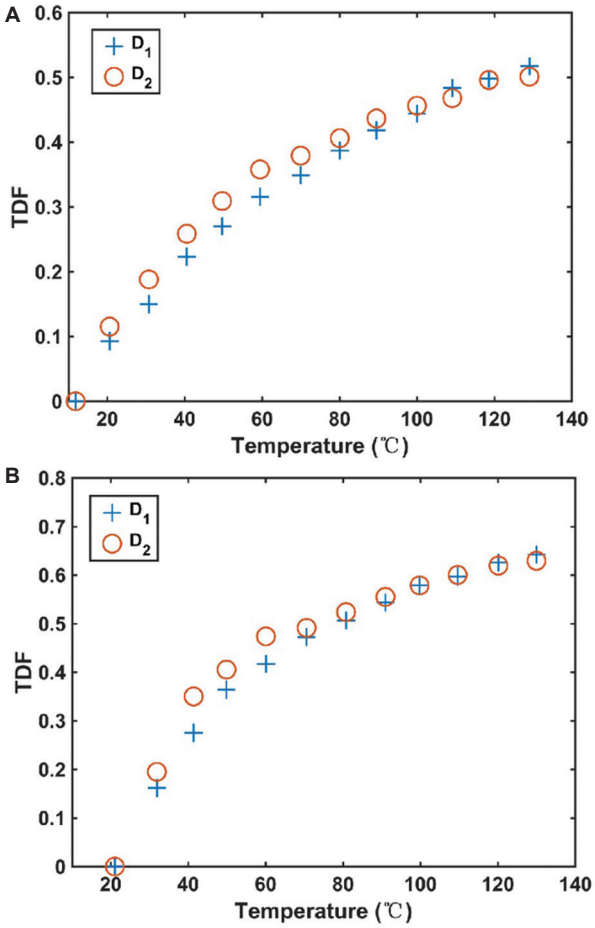

Figure 3. Thermal damage factors (TDFs) of (A) Sample 1 and (B) Sample 2 as a function of temperature under a confining pressure of 5.93 MPa. Data from Yuan *et al.*[31]

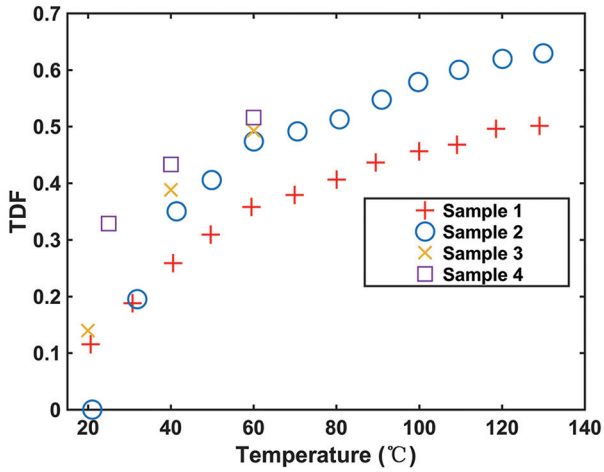

Figure 4. Thermal damage factors (TDFs) of samples as a function of temperature. The data for Samples 1 and 2 were from Yuan *et al.*[31] under a confining pressure of 5.93 MPa, while those for Samples 3 and 4 were from Li *et al.*[41] under a confining pressure of 7.58 MPa.

the presence of heavy oil causes the higher values in the rock. Moreover, the properties of Sample 3 were more dependent on the properties of heavy oil. Therefore, the velocities of Sample 3 were more sensitive to temperature. When the samples were saturated with the same heavy oil, the TDF of Sample 2 was higher than that of Sample 1, indicating that porosity also has an impact on rock damage (a similar trend is observed when comparing with Samples 3 and 4). It is known that the response of oil sand to temperature reflects the combined effect of the heavy oil and the rock frame.[47]

3.2. Effect of pressure on thermal damage factor

When the rock frame is subjected to confining pressure, the influence of pressure should be considered during the heat-extraction process. The experimental data of oil sands reported by Li *et al.*[41] were used to analyze the effects of temperature and pressure on the thermal damage in three artificial oil sand samples (Samples 3, 4, and 5). The properties are provided in Table 1.

For the three samples at different confining pressures, Figure 5 depicts how V_P/V_S varies with temperature. From Figure 5, we observed that V_P/V_S showed a trend of first increasing and then decreasing. This is because the heavy oil was in the quasi-solid phase. With increasing temperature, the rate of decline for S-wave velocity was more significant than that for P-wave velocity. When the temperature exceeded the liquid point, the S-wave velocity was almost unchanged, but the P-wave velocity continued to decrease, causing a decreasing trend in the V_P/V_S ratio. This indicates that heavy oil may have no significant impact on the S-wave velocity for the liquid phase. It has been demonstrated that pressure affects the properties of rocks.[31,46,48] When the temperature was constant and the confining pressure increased, V_P/V_S decreased, especially for heavy oil in the fluid phase, indicating that the samples became stiffer at higher pressure. For Samples 3, 4, and 5, which have larger porosities, soft cracks are more easily closed under pressure.[49] As a result, the velocities increase significantly.

We used dry Sample 3 as an example in Figure 6 to show velocities as a function of pressure with an exponential law of the Shapiro type[50] at room temperature (Figure 6A). Subsequently, fluid substitution was performed with heavy oil using the EG equation, and the results were compared with experimental data (Figure 6B). From the figure, it is evident that the increase in the velocity of the dry samples with pressure reflects the closure of cracks and pores within the rock. As pressure increased, the rock's elastic moduli increased, resulting in higher wave velocities. Furthermore, pressure has an effect on the velocities of wet samples. We

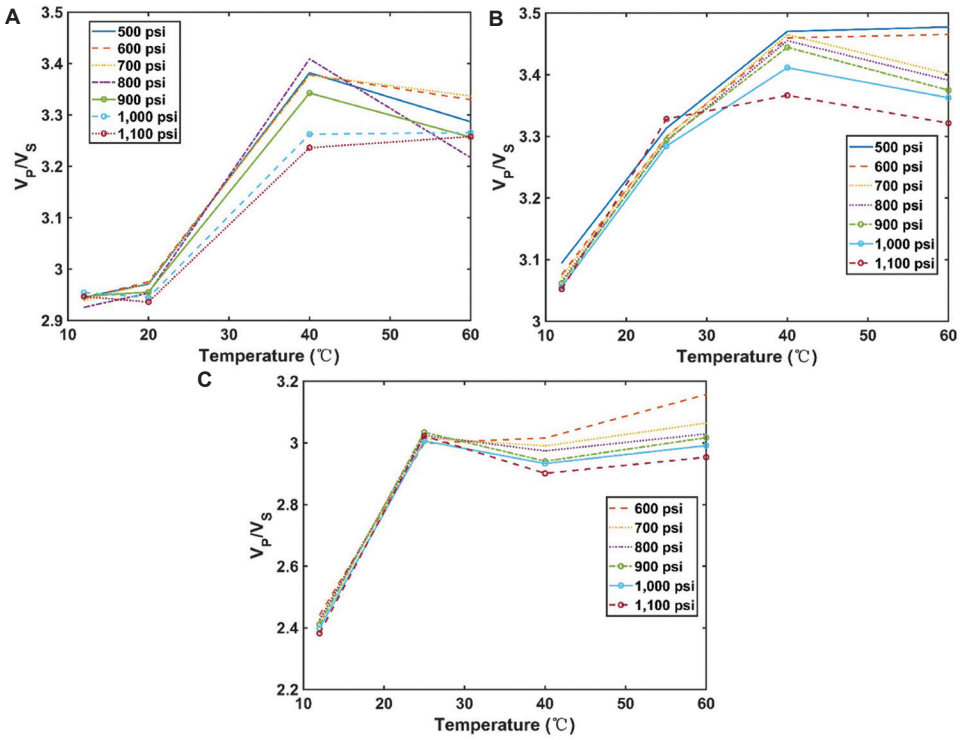

Figure 5. V_P/V_S as a function of temperature with different confining pressures in (A) Sample 3, (B) Sample 4, and (C) Sample 5. Data from Li *et al.*[41]

considered **Equation 9** to calculate TDFs of Samples 3, 4, and 5 to analyze the effect of confining pressure on TDF. As seen in Figure 7, TDF tended to decrease as the confining pressure increased. This is due to the fact that the velocities increase with pressure. Moduli of rock increase under higher pressures, and the rock becomes a stiffer medium, making it less prone to damage at the same temperature.

4. Thermal damage factors of dry and heavy oil rocks

Sample 6 (in Table 1) tested in Han *et al.*[25] was selected for analysis. The pore fluid was heavy oil characterized by 9.2° API density and a liquid point of approximately 60°C. During the test, the pore pressure was maintained at 2.4 MPa. The oil sand Sample 7, reported by Li *et al.*,[45] was also considered. The sample was composed of silt-size grains, which mainly consist of quartz, with minor amounts of clay, feldspar, and plagioclase. The pore fluid is heavy oil with a 6.9° API density and 49°C liquid point. During the experiment, the pore pressure was set to 3.5 MPa.

4.1. Estimation of the thermal damage factor of heavy oil-saturated rocks

Temperature-dependent velocities of dry and oil-saturated samples for Samples 6 and 7 are shown in Figure 8. The velocities of the wet samples were significantly higher than those of the dry ones. When the liquid point was exceeded, the P-wave velocity gradually decreased, while the S-wave velocity remained constant, indicating that the heavy oil exists in a fluid state and that the rock velocity is mainly affected by the frame, crack, and fluid bulk modulus and density.[25,40]

Figure 9 shows the TDFs of dry and oil-sand samples. As can be seen, the trends were similar to those in Figure 4. The thermal damage in oil sands under varying temperatures was more pronounced than in the dry samples, suggesting that the transition of heavy oil to a fluid state reduces rock stiffness and increases damage as temperature rises.[43]

By assuming that TDFs of the dry rocks were known (Samples 6 and 7), fluid substitution was carried out by combining the EG and Maxwell models to estimate TDFs of the wet rocks. The resulting data were compared with the actual results. Figure 10 shows that the model results are in good agreement with the experimental data, validating that the proposed method can effectively account for TDFs of oil sands with respect to temperature.

Then, we considered Sample 7 to analyze the dependence of the dry- and wet-rock moduli with respect to temperature (Figure 11). As can be seen, the wet-rock bulk modulus exhibited a more pronounced variation. Meanwhile, with increasing temperature, the wet-rock shear modulus approached that of the dry samples, as expected.

4.2. Thermal damage factor threshold

Han *et al.*[40] proposed a fluid viscosity threshold, specifically the liquid point, to explain the non-linear velocity behaviors of P- and S-waves. The normalized temperature is defined as:

$$T_n = \frac{T_w - T}{T_w - T_g} \tag{25}$$

where T_w refers to the temperature when the viscosity of fluid is equivalent to the viscosity of water, which is 1 cP; and T_g denotes the fluid glass point, defined as the temperature at which the viscosity reaches 10^{15} cP.

Figure 12 illustrates the relationship between TDFs and normalized temperature for Samples 6 and 7. The liquid points corresponded to $T_n = 0.86$ and 0.77 in Figure 12A and B, respectively, indicating the threshold between the linear and non-linear behaviors of TDF. These findings show that the viscosities of different fluids have varying effects on the TDFs of oil sands, whereas the porosity of rock samples has no evident influence on this threshold.

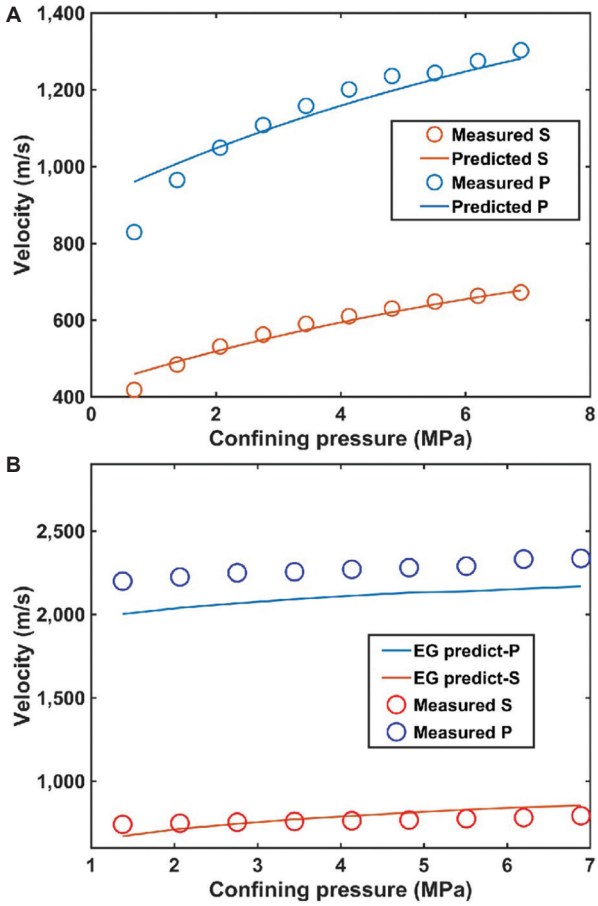

Figure 6. Predicted and measured velocities of (A) dry and (B) wet Sample 3 as a function of confining pressures at room temperature. Data from Li *et al.*[41]
Abbreviation: EG: Extended Gassmann.

5. Discussion

In this study, the thermal response of elastic wave velocities in oil sands reflects the coupled effects among mineral grains, pore fluids, and cracks with temperature variations. As shown in Figure 8 for Samples 6 and 7, both P- and S-wave velocities exhibited varying degrees of reduction with increasing temperature, indicating that as the temperature increases, the fluid properties, microstructure, and mechanical characteristics of oil sands undergo significant changes. The estimated TDF model was established based on wave velocity variations, the generalized Gassmann equations, and the Maxwell model. It effectively characterizes these thermally induced effects and provides a quantitative description of the initial stage of thermal damage.

Within the temperature range below the liquid point (approximately below 60°C for Sample 6 and 49°C for Sample 7), both P- and S-wave velocities showed a rapid and slightly non-linear decrease with increasing temperature. This stage mainly reflects the softening and partial flow of heavy oil, as well as the thermal expansion effect of pore fluids. At room temperature, heavy oil acts

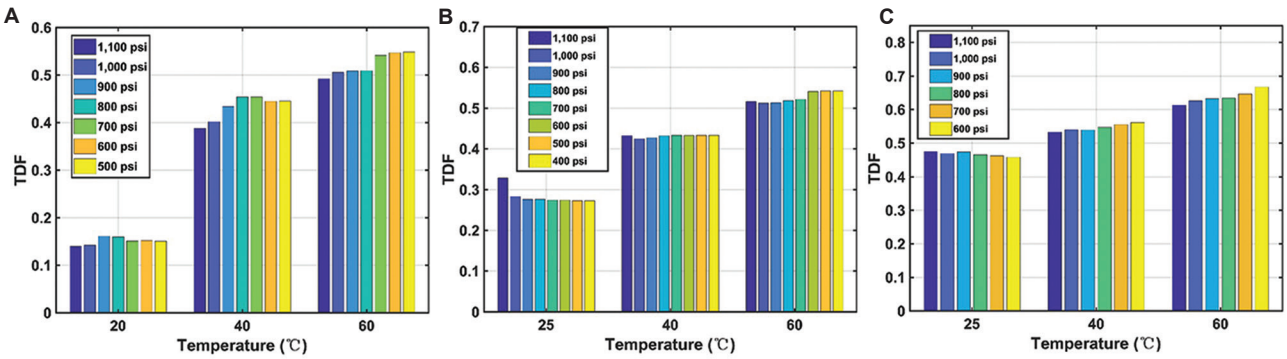

Figure 7. Thermal damage factors (TDFs) of (A) Sample 3, (B) Sample 4, and (C) Sample 5 at different confining pressures as a function of temperature

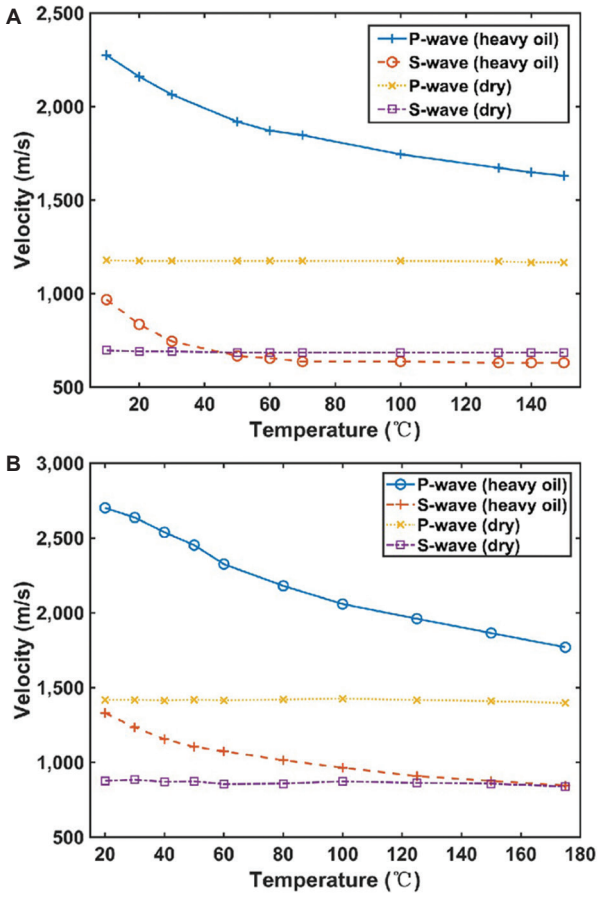

Figure 8. The velocities of dry and heavy oil samples of (A) Sample 6 and (B) Sample 7 as a function of temperature. Data of Sample 6 from Han *et al.*[25] under the confining pressure of 8 MPa, and Data of Sample 7 from Li *et al.*[45] under the confining pressure of 7 MPa.

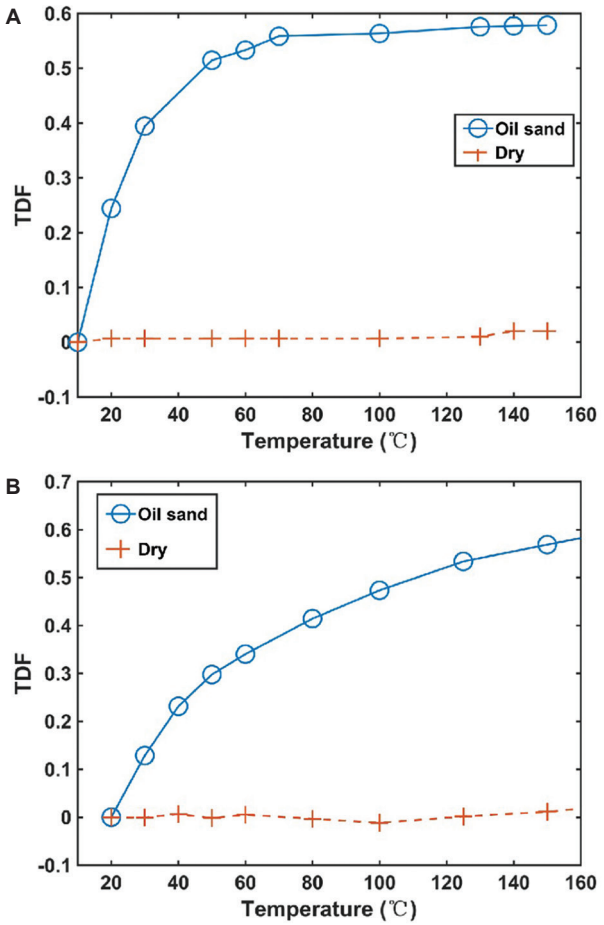

Figure 9. Thermal damage factors (TDFs) of (A) Sample 6 and (B) Sample 7 as a function of temperature under the confining pressures of 8 MPa and 7 MPa, respectively. Data of Sample 6 from Han *et al.*[25] and data of Sample 7 from Li *et al.*[45]

as a viscoelastic medium, providing bonding and support for mineral grains. As the temperature rises, its viscosity decreases significantly, weakening the contact stiffness and cementation strength between grains.[51] This causes a decrease in the rock's bulk modulus and shear modulus, leading to a reduction in the velocities of P-waves and S-waves. The heavy oil undergoes a continuous transition from a viscoelastic solid to a fluid. As the temperature increases, the relaxation time of heavy oil shortens significantly,[52] and its stress-bearing capacity at grain contacts weakens, leading to a gradual non-linear trend in the TDF–temperature relationship (Figures 9 and 10).

At higher temperature stages (approximately 160°C), the decreasing trend of P- and S-wave velocities became nearly linear. The decreasing rate of S-wave velocity was significantly lower than that in the low-temperature stage, indicating a notable reduction in the sensitivity of shear stiffness to temperature. From the comparison results of P-waves and S-waves, it can be observed that with

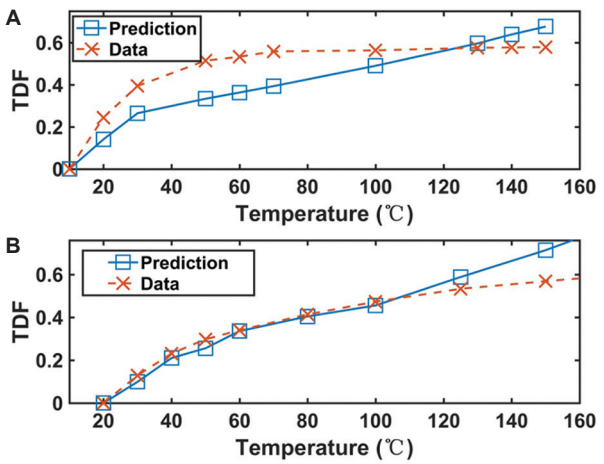

Figure 10. Predicted and measured results of thermal damage factors (TDFs) of oil sands as a function of temperature for (A) Sample 6 and (B) Sample 7 under the confining pressures of 8 MPa and 7 MPa, respectively. Data of Sample 6 from Han *et al.*[25] and data of Sample 7 from Li *et al.*[45]

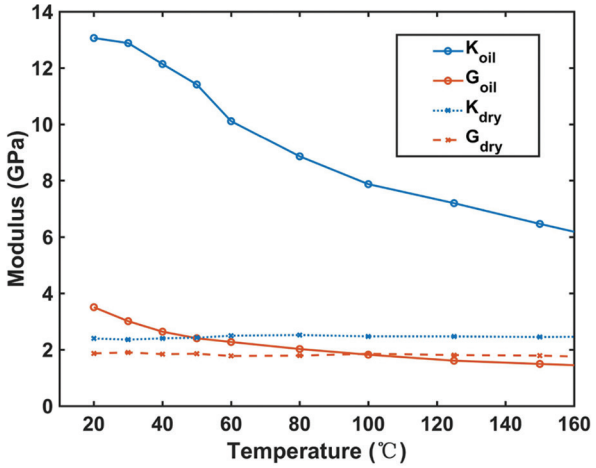

Figure 11. Dry- and wet-rock moduli as a function of temperature for Sample 7 under the confining pressure of 7 MPa. Data of Sample 7 from Li *et al.*[45]

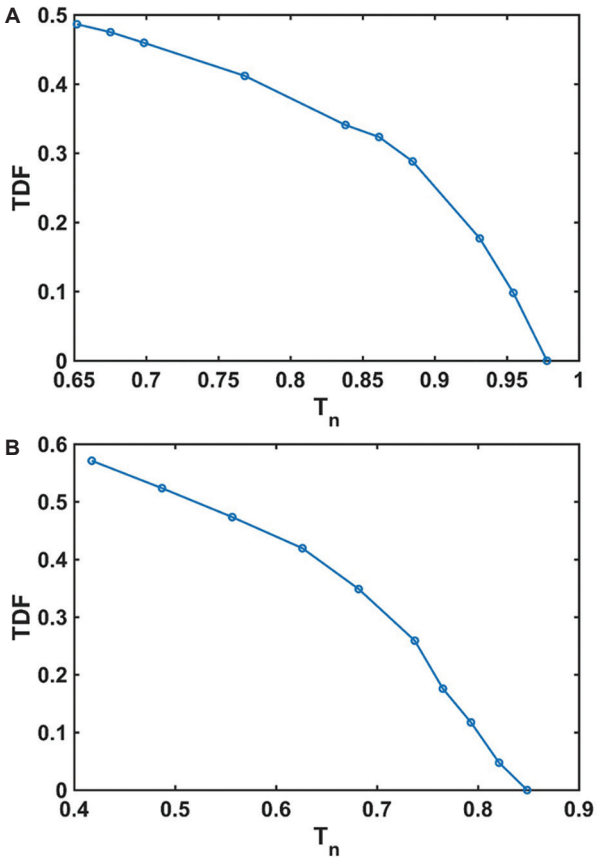

Figure 12. Thermal damage factors (TDFs) for (A) Sample 6 and (B) Sample 7 as a function of the normalized temperature (T_n) under the confining pressure of 8 MPa and 7 MPa, respectively

increasing temperature, the shear modulus tended to stabilize, whereas the bulk modulus continued to decline (Figure 11). This stage corresponds to the complete transformation of heavy oil into a fluid phase that fills the pore–crack space. The thermal expansion mismatch among mineral components generates localized thermal stresses, promoting the initiation and propagation of microcracks.[44] The effect of increasing temperature on S-wave propagation is limited; as a result, the decreasing trend of S-wave velocity slows down, while P-wave velocity becomes more sensitive to temperature.

The TDFs calculated from the proposed model further illustrate the characteristics of this fluid-dominated stage. When the temperature exceeds the liquid point, the TDF–temperature relationship gradually shows a linear trend (Figures 9 and 10). The fitted results of the proposed model are generally consistent with the trend of TDFs calculated from experimental wave velocities, indicating that the model can effectively capture the thermally induced stiffness evolution of heavy oil sands in both quasi-solid and fluid states. Within the temperature range of this study, the TDF can serve as a quantitative indicator to describe the thermal weakening of elastic moduli.

Overall, the results indicate that even below the mineral decomposition threshold, elastic wave velocity variations remain a sensitive indicator of thermally induced mechanical changes in oil sands. The proposed model provides an effective quantitative framework to characterize these changes and offers valuable theoretical insights into the elastic wave propagation behavior of oil sands under thermal recovery or thermal simulation conditions. Future research may extend the investigation to higher temperature ranges and real reservoir monitoring environments to further validate and refine the proposed model.

6. Conclusion

The physical properties of heavy oil-bearing rocks are affected by temperature, as the pore filling is solid at low temperatures and fluid at higher temperatures under certain conditions. Two definitions of TDF, derived from different wave-velocity formulations, were compared in this study. We also considered the variations of TDFs with respect to varying confining pressure. The theoretical model was established based on the generalized Gassmann equations for a solid pore filling with the viscoelastic Maxwell model, which describes the temperature-dependent properties of heavy oil. For both dry and wet rocks, the model effectively describes their TDFs as a function of temperature and agrees with laboratory measurements on oil sands. The findings of this study may help clarify the thermal damage behaviors of oil sands and contribute to optimizing heavy-oil thermal recovery by improving the accuracy of reservoir prediction and evaluation. The proposed model further supports thermal-recovery monitoring and

oil-sand numerical simulation by linking temperature-dependent velocity variations to underlying viscoelastic and thermal damage mechanisms, enhancing its scientific and engineering practicality.

Acknowledgments

None.

Funding

This work was supported by the National Natural Science Foundation of China (grant no.: 42174161, 42404120, and 42504128), the research fund of North China University of Water Resources and Electric Power (grant no.: 202209020), and the Natural Science Foundation of Henan (grant no.: 242300421461).

Conflict of interest

Jing Ba is an Editorial Board Member of this journal, but was not in any way involved in the editorial and peer-review process conducted for this paper, directly or indirectly. Wenhao Xu is an employee of China National Petroleum Corporation; however, he was not involved in any activities that could constitute a conflict of interest in relation to this study. The authors declare that they have no known competing financial interests or personal relationships that could have appeared to influence the work reported in this paper.

Author contributions

Conceptualization: Hui Qi, Jing Ba
Formal analysis: Wenhao Xu
Investigation: Yuanyuan Huo, Jishun Pan, Qingchun Jiang, Congsheng Bian
Methodology: Hui Qi, Jing Ba
Writing–original draft: Hui Qi, Jing Ba
Writing–review & editing: Hui Qi, Jing Ba, Wenhao Xu

Availability of data

The data that support the findings of this study are available from the corresponding author upon reasonable request.

References

1. Jiang Q, You H, Pan J, *et al*. Preliminary discussion on current status and development direction of heavy oil recovery technologies. *Special Oil Gas Reserv*. 2020;27(6):30-39.

   doi: 10.3969/j.issn.1006-6535.2020.06.004

2. Yu X, Liu X, Chen M, Wu G, Li X. Study on influence of heavy oil reservoir damage caused by multi-component thermal fluid huff and puff. *Front Energy Res*. 2022;10:821221.

   doi: 10.3389/fenrg.2022.821221

3. Kudrashou VY, Nasr-El-Din HA. Formation damage associated with mineral alteration and formation of swelling clays caused by steam injection in sand packs. *SPE Reservoir Eval Eng*. 2020;23(1):326-344.

   doi: 10.2118/195700-PA

4. Yuan H, Han D, Li H, Zhao L, Zhang W. The effect of rock frame on elastic properties of bitumen sands. *J Petrol Sci Eng*. 2020;194:107460.

   doi: 10.1016/j.petrol.2020.107460

5. Zhao DW, Wang J, Gates ID. Thermal recovery strategies for thin heavy oil reservoirs. *Fuel*. 2014;117:431-441.

   doi: 10.1016/j.fuel.2013.09.023

6. Zhuang Y, Liu X, Xiong H, Liang L. Microscopic mechanism of clay minerals on reservoir damage during steam injection in unconsolidated sandstone. *Energy Fuels*. 2018;32(4):4671-4681.

   doi: 10.1021/acs.energyfuels.7b03686

7. Dong X, Liu H, Chen Z, Wu K, Lu N, Zhang Q. Enhanced oil recovery techniques for heavy oil and oilsands reservoirs after steam injection. *Appl Energy*. 2019;239:1190-1211.

   doi: 10.1016/j.apenergy.2019.01.244

8. Li F, Zhou H, Zhao T, Marfurt KJ. Unconventional reservoir characterization based on spectrally corrected seismic attenuation estimation. *J Seism Explor*. 2016;25(5):447-461.

9. David C, Menéndez B, Darot M. Influence of stress-induced and thermal cracking on physical properties and microstructure of La Peyratte granite. *Int J Rock Mech Min Sci*. 1999;36(4):433-448.

   doi: 10.1016/S0148-9062(99)00010-8

10. Hassanzadegan A, Blöcher G, Milsch H, Urpi L, Zimmermann G. The effects of temperature and pressure on the porosity evolution of Flechtinger sandstone. *Rock Mech Rock Eng*. 2014;47(2):421-434.

    doi: 10.1007/s00603-013-0401-z

11. Xi DY, Xu SL, Tao YZ, Li T. Experimental investigations of thermal damage for rocks. *Key Eng Mater*. 2006;324:1213-1216.

    doi: 10.4028/www.scientific.net/KEM.324-325.1213

12. Zhang W, Sun Q, Hao S, Wang B. Experimental study on the thermal damage characteristics of limestone and underlying mechanism. *Rock Mech Rock Eng*. 2016;49(8):2999-3008.

    doi: 10.1007/s00603-016-0983-3

13. Zhang W, Sun Q, Zhu S, Wang B. Experimental study on mechanical and porous characteristics of limestone affected by high temperature. *Appl Therm Eng*. 2017;110:356-362.

    doi: 10.1016/j.applthermaleng.2016.08.194

14. Dougill JW, Lau JC, Burt NJ. *Toward a Theoretical Model for Progressive Failure and Softening in Rock. Concrete and*

Similar Material. Canada: University of Waterloo Press; 1977.

15. Trippetta F, Ruggieri R, Motra HB. Temperature and pressure effects on the mechanical behavior of porous carbonates saturated by viscous fluids. *Int J Rock Mech Min Sci*. 2024;183:105938.

    doi: 10.1016/j.ijrmms.2024.105938

16. Sirdesai NN, Singh A, Sharma LK, Singh R, Singh TN. Determination of thermal damage in rock specimen using intelligent techniques. *Eng Geol*. 2018;239:179-194.

    doi: 10.1016/j.enggeo.2018.03.027

17. Sun H, Sun Q, Deng W, Zhang WQ, Chao L. Temperature effect on microstructure and P-wave propagation in Linyi sandstone. *Appl Therm Eng*. 2017;115:913-922.

    doi: 10.1016/j.applthermaleng.2017.01.026

18. Yao M, Rong G, Zhou C, Peng J. Effects of thermal damage and confining pressure on the mechanical properties of coarse marble. *Rock Mech Rock Eng*. 2016;49(6):2043-2054.

    doi: 10.1007/s00603-016-0916-1

19. Zhu S, Zhang W, Sun Q, Deng S, Geng J, Li C. Thermally induced variation of primary wave velocity in granite from Yantai: Experimental and modeling results. *Int J Therm Sci*. 2017;114:320-326.

    doi: 10.1016/j.ijthermalsci.2017.01.008

20. Yang J, Fu LY, Zhang W, Wang ZW. Mechanical property and thermal damage factor of limestone at high temperature. *Int J Rock Mech Min Sci*. 2019;117:11-19.

    doi: 10.1016/j.ijrmms.2019.03.012

21. Batzle M, Hofmann R, Han DH. Heavy oils-seismic properties. *Lead Edge*. 2006;25(6):750-756.

    doi: 10.1190/1.2210074

22. Rabbani A, Schmitt DR, Nycz J, Gray K. Pressure and temperature dependence of acoustic wave speeds in bitumen-saturated carbonates: Implications for seismic monitoring of the Grosmont Formation. *Geophysics*. 2017;82(5):MR133-MR151.

    doi: 10.1190/geo2016-0667.1

23. Xi D, Liu X, Zhang C. The frequency (or time)-temperature equivalence of relaxation in saturated rocks. *Pure Appl Geophys*. 2007;164(11):2157-2173.

    doi: 10.1007/s00024-007-0270-z

24. Han DH, Yao Q, Zhao H. Complex properties of heavy oil sand. *SEG Int Expos Ann Meet*. 2007;26:1609-1613.

    doi: 10.1190/1.2792803

25. Han DH, Zhao H, Yao Q, Batzle M. Velocity of heavy-oil sand. *Soc Explor Geophys*. 2007;26:1619-1623.

    doi: 10.1190/1.2792805

26. Butler RM. *Thermal Recovery of Oil and Bitumen*. Englewood Cliffs, New Jersey: Prentice Hall Publishing Company; 1991.

27. Gates ID, Adams J, Larter S. The impact of oil viscosity heterogeneity on the production characteristics of tar sand and heavy oil reservoirs. Part II: Intelligent, geotailored recovery processes in compositionally graded reservoirs. *J Can Petrol Technol*. 2008;47(09):40-49.

    doi: 10.2118/08-09-40

28. Han DH. *Thermal Damage on Velocities of Heavy Oil Sands*. SEG International Exposition and Annual Meeting (SEG); 2012.

29. Pang ZX, Liu HQ, Liu XL. Characteristics of formation damage and variations of reservoir properties during steam injection in heavy oil reservoir. *Petrol Sci Technol*. 2010;28(5):477-493.

    doi: 10.1080/10916460902780335

30. He Y, Niu W, Gao Z, *et al*. Adsorption behavior of asphaltene on clay minerals and quartz in a heavy oil sandstone reservoir with thermal damage. *Clays Clay Miner*. 2022;70(1):120-134.

    doi: 10.1007/s42860-022-00178-5

31. Yuan H, Han DH, Zhang W. Heavy oil sands measurement and rock-physics modeling. *Geophysics*. 2016;81(1):D57-D70.

    doi: 10.1190/geo2014-0573.1

32. Wolf K, Mukerji T, Mavko G. *Attenuation and Velocity Dispersion Modeling of Bitumen Saturated Sand. SEG International Exposition and Annual Meeting*. SEG, 2006.

33. Ciz R, Shapiro SA. Generalization of Gassmann equations for porous media saturated with a solid material. *Geophysics*. 2007;72(6):A75-A79.

    doi: 10.1190/1.2772400

34. Ciz R, Saenger EH, Gurevich B, Shapiro SA. Temperature-dependent poroelastic and viscoelastic effects on microscale-modelling of seismic reflections in heavy oil reservoirs. *Geophys J Int*. 2009;176(3):822-832.

    doi: 10.1111/j.1365-246X.2008.04016.x

35. Carcione JM, Helle HB, Avseth P. Source-rock seismic-velocity models: Gassmann versus Backus. *Geophysics*. 2011;76(5):N37-N45.

    doi: 10.1190/geo2010-0258.1

36. Carcione JM. Wave fields in real media. In: *Theory and Numerical Simulation of Wave Propagation in Anisotropic. Anelastic, Porous and Electromagnetic Media*. Netherlands: Elsevier; 2007.

37. Zhao HB, Yin GZ, Chen LJ. Experimental study on effect of temperature on sandstone damage. *Chin J Rock Mech Eng*. 2009;28(1):2784-2788.

38. Mukerji T, Dvorkin J. *The Rock Physics Handbook: Tools for Seismic Analysis in Porous Media*. Cambridge: Cambridge University Press; 1998.

39. Lan HT, Chen SM, Chi HZ, Pei JY, Lin W, Shen JG. A viscoelastic representation of seismic wave attenuation and dispersion caused by wave-induced fluid flow in fractured porous media. *J Seism Explor*. 2020;29(6):587-601.

40. Han D, Liu J, Batzle M. Seismic properties of heavy oils-measured data. *Lead Edge*. 2008;27:1108-1115.

doi: 10.1190/1.2978972

41. Li H, Zhao L, Han DH, Sun M, Zhang Y. Elastic properties of heavy oil sands: Effects of temperature, pressure, and microstructure. *Geophysics*. 2016;81(4):D453-D464.

doi: 10.1190/geo2015-0351.1

42. Qi H, Ba J, Carcione JM, Zhang L. Temperature-dependent wave velocities of heavy oil-saturated rocks. *Lithosphere*. 2022;2021(Special 3):3018678.

doi: 10.2113/2022/3018678

43. Liu HF, Xu YY, Chen H, Zhang J, Xu JY. Viscoelastic behavior and constitutive relation of heavy crude oils. *ACS Omega*. 2022;7(35):30816-30822.

doi: 10.1021/acsomega.2c02234

44. Fredrich JT, Wong T. Micromechanics of thermally induced cracking in three crustal rocks. *J Geophys Res Solid Earth*. 1986;91(B12):12743-12764.

doi: 1029.091/JB12iB12743p389

45. Li H, Han D, Sun M, Yuan HM, Gao JH. An experimental investigation on effects of saturation levels and fluid types on elastic properties of bitumen-saturated sands at elevated temperatures. *Energy*. 2022;238:122011.

doi: 10.1016/j.energy.2021.122011

46. Yuan H, Wang Y, Han D, Li H, Zhao L. Velocity measurement of North Sea heavy oil sands under changing pressure and temperature. *J Petrol Sci Eng*. 2021;205:108825.

doi: 10.1016/j.petrol.2021.108825

47. Nie J, Han X, Geng J. Temperature-dependent rock physics modeling for heavy oil sands. *J Petrol Sci Eng*. 2022;215:110642.

doi: 10.1016/j.petrol.2022.110642

48. Yuan H, Han D. *Pressure and Temperature Effect on Heavy Oil Sands Properties. SEG International Exposition and Annual Meeting*. SEG; 2013.

49. Wei Y, Ba J, Carcione JM. Stress effects on wave velocities of rocks: Contribution of crack closure, squirt flow and acoustoelasticity. *J Geophys Res Solid Earth*. 2022;127(10):e2022JB025253.

doi: 1029.2022/025253JB15

50. Ma ZG, Wu XY, Wang ZH. Effect of effective pressure on compressional and shear wave velocities. *Prog Explor Geophys (Chin)*. 2006;29(3):183-186.

51. Guo J, Han X. Rock physics modelling of acoustic velocities for heavy oil sand. *J Petrol Sci Eng*. 2016;145:436-443.

doi: 10.1016/j.petrol.2016.05.028

52. Makarynska D, Gurevich B, Behura J, Batzle M. Fluid substitution in rocks saturated with viscoelastic fluids. *Geophysics*. 2010;75(2):E115-E122.

doi: 10.1190/1.3360313